Comparison of cellular changes in cavalier King Charles spaniel and mixed breed dogs with myxomatous mitral valve disease

Comparison of cellular changes in cavalier King Charles spaniel and mixed breed dogs with myxomatous mitral valve disease

Chi-Chien Lu DVM[a], Meng-Meng Liu PhD [a], Geoff Culshaw BVM&S[a], Anne French PhD[b], Brendan Corcoran PhD[a]

[a]Royal (Dick) School of Veterinary Studies and The Roslin Institute, the University of Edinburgh, Easterbush, Roslin, Mid-Lothian, Scotland, UK EH25 9RG.

[b]School of Veterinary Medicine, the University of Glasgow, Garscube Campus Bearsden Road, Glasgow, Scotland, UK G61 1QH.

*Corresponding Author: Brendan Corcoran. E-mail; Brendan.Corcoran@ed.ac.uk

Abstract

Objectives: The aim of this study was to determine if there are differences in cellular changes in cavalier King Charles spaniel (CKCS) myxomatous mitral valves compared to non-CKCS dogs.

Animals: CKCSs (n=6) and age-matched mixed breed (n=6) with severe MMVD, and normal mixed breed (n=4) dogs.

Methods: Immunohistochemistry staining and qualitative and quantitative analysis of mitral valves sections, examining for the presence of CD11c and CD45, vimentin, alpha smooth muscle actin (α-SMA) and myosin heavy chain 10 (Smemb), vonWillebrand factor (vWF) and CD31 and Ki-67.

Results: Vimentin positive cell numbers were increased in the MMVD dogs and distributed throughout the valve with greatest density close to the endothelium. There were no significant differences in cell marker expression for the two diseased groups, but cell numbers were significantly increased compared to controls for α-SMA (CKCS only) and SMemb (CKCS and mixed breed) (P<0.05). α-SMA+ cells were primarily located at the valve edge, with Smemb+ cells similarly located, but also present throughout the valve stroma. A small number of cells close to the valve edge co-expressed α-SMA and SMemb. Endothelial vWF expression was identified in all valves, with evidence of disrupted endothelium in the diseased, but was also found in diseased valve stroma. There was no staining for CD11c, CD45 or CD31 in any valve. Ki-67+ cells formed linear clusters at the leaflet tip and were sparsely distributed throughout both myxomatous valve groups.

Conclusions: The cellular changes notes with advanced stage MMVD are appear similar for CKCS when compared to mixed breed dogs.

Key words: Canine, Cellularity, Endothelial, Immunohistochemistry, Interstitial.

Abbreviations:

CKCS	cavalier King Charles spaniel
MMVD	myxomatous mitral valve disease
5-HT	5-hydroxytryptamine (serotonin)
α-SMA	alpha smooth muscle actin
VIC	valve interstitial cell
MYH-10	myosin heavy chain 10 (SMemb)
Non-muscle embryonic myosin	SMemb (MYH-10)
VEC	valve endothelial cell
PBS	phosphate-buffered saline
vWF	von Willebrand Factor
DAPI	4',6-diamidino-2-phenylindole
ANOVA	one-way analysis of variance

Introduction:

The cavalier King Charles spaniel (CKCS) breed is recognised to be particularly predisposed to the development of myxomatous mitral valve disease (MMVD) in terms of age of onset, progression and severity[1-3]. MMVD is highly heritable in the CKCS breed and it is reasonable to suppose heritability also has a role in disease appearance and progression [4,5]. There are CKCS-specific traits such as differences in platelet numbers and platelet aggregation tendency and higher serum magnesium and 5-HT (serotonin) levels compared to other dogs that have been examined for correlation with development of MMVD, with varying results[6-12]. Furthermore, the CKCS is more predisposed to chronic fibrosing pancreatitis and syringomyelia than other

65 breeds and with MMVD this might reflect a breed-specific global connective tissue
66 abnormality[13-15]. While there is no clear causal link established between these findings
67 in the CKCS and MMVD it still points towards breed-specific phenotypic
68 characteristics that might have bearing on disease appearance.
69
70 Cellular changes that occur with MMVD are well described. There is an increase in α-
71 smooth muscle actin (α-SMA) positive valve interstitial cells (activated
72 myofibroblasts, aVICs) which locate mainly towards the valve distal free-edge (valve
73 tip) and appears to be related to disease severity[16-19]. It is activation of the VICs that is
74 believed to drive the extra-cellular matrix damage seen in MMVD through a
75 combination of increased catabolic activity and aberrant repair and replacement. In
76 normal valve stroma the majority of cells are quiescent vimentin-positive VICs
77 (qVIC), with a few desmin-positive cells [16, 17]. In overtly myxomatous areas of
78 affected valves some cells also appear to be activated myofibroblasts or with
79 increased differentiation capacity based on their expression of myosin heavy chain-10
80 (MYH-10; non-muscle embryonic myosin, SMemb), with appearance of cells in
81 clusters close to the endothelium and deeper in the valve stroma[20, 21]. There is no
82 evidence that there is active cell proliferation and while some cells exhibit a pro-
83 apoptotic status they do not undergo programmed cell death[16, 22]. However, there are
84 regional changes in cell numbers; reduced in overtly myxoid stroma and increased in
85 sub-endothelial zones[21]. A small increase in mast cell numbers is also noted, but there
86 is no increase in macrophages numbers and no inflammatory cells are reported[16, 17].
87 Changes in endothelial cell morphology, coupled with endothelial cell (VEC) loss are
88 also reported[16, 23, 24]. Changes include increased expression of endothelin receptors,
89 evidence of VEC activation, apoptosis, basement membrane loss and damage with

cell detachment [25,26]. The interaction between the VECs and VICs in the context of the pathogenesis of MMVD is not understood, but the characteristic accumulation of activated myofibroblasts close to the endothelium and in particular areas of damaged endothelium suggest some sort of interaction does occur [26].

Of the studies to date, all have presented data from a mix of pedigree and cross-bred dogs. Considering the susceptibility of the CKCS to MMVD, the aim of this study was to determine if there are differences in valve cellular changes in the CKCS compared to non-CKCS dogs examining the resident valve interstitial and endothelial cells, to confirm the cell changes noted in previous studies and also examine again for the possible presence of inflammatory cells and macrophages.

Animals, Materials and Methods:

Tissue samples

Anterior mitral valve leaflets were obtained from six elderly CKCS (12-14 yr; 2 neutered females & 4 neutered males; 8-12 Kg) and six mixed breed dogs (8-12 yr; 3 neutered females & 3 neutered males; 10-18Kg) with MMVD. Control samples were obtained from four young adult mixed breed dogs (1-2 yr; 2 intact males & 2 neutered females; 12-15kg) with no evidence of disease. All samples were collected with full owner consent and the study conformed to national (UK) and institutional ethical guidelines for the use of animals in research. Valves were removed within minutes of death, gently washed with phosphate-buffered saline (PBS), immersed in 4% paraformaldehyde and stored at 4° C for 36 hr. Samples were then rinsed in PBS and stored in 70% ethanol at 4° C until required. Valves were pathologically graded Whitney Grade 3 or 4 by at least two of the authors independently at the time of

115 collection and then a grade agreed (C-CL, BMC, M-ML & GJC)[27]. Representative
116 samples of similar gross pathological appearance were cut from each valve, paraffin-
117 embedded and 4 consecutive 5 μm sections were collected onto coated slide. Whole
118 valve length and distal transverse sections were collected for longitudinal and
119 horizontal evaluation. Sections were de-waxed in xylene and re-hydrated through
120 serial ethanols and distilled water.
121
122 *Immunohistochemistry*
123 Immunohistochemical staining used a combination of a standard peroxidase method
124 (qualitative) with NovaRed[c] as chromagen ~~(ABC Elite Kit, Vector)~~, and indirect
125 immunofluorescence (qualitative and quantitative) using fluorescent dyes conjugated
126 to IgG[d] ~~(AlexaFluor488 and 568, Invitrogen)~~. Double staining was carried out for α-
127 SMA and SMemb using indirect immunofluorescence to determine if there was co-
128 localisation. ~~For double staining~~ Images were collected using the two different
129 fluorescence channels and then merged. Sections were examined using fluorescence
130 and light microscopy[e] ~~(Leica DMRB)~~ for the presence of the universal mesenchymal
131 cell marker vimentin, the inflammatory cell markers CD11c (macrophage, monocytes)
132 and CD45 (hematopoietic cells, T-cell lymphocytes), the valve endothelial cell (VEC)
133 markers vWf and CD31, the activated myofibroblasts (aVIC) markers α-smooth
134 muscle actin (α-SMA), myosin heavy chain-10 (SMemb) and the cell proliferation
135 marker Ki67. The details for each antibody are shown in Table 1. For antigen retrieval
136 sections were microwaved either in citrate buffer (0.01 M, pH 6.0) or Tris-EDTA
137 (10mM Tris base, 1 mM EDTA solution, pH 8.0).
138

For the peroxidase technique sections were incubated with 1% hydrogen peroxide (H_2O_2 in phosphate-buffered saline (PBS pH 7.4) for 10 min and blocked with 10% goat serum ~~(~~diluted in 0.5% Tween 20~~)~~[f]) ~~(Vector Laboratories Inc.)~~ for 30 min at room temperature. Sections were then incubated for 60 min at room temperature with primary antibodies, rinsed in 0.5% Tween20 in PBS and incubated for 30 min at room temperature with biotinylated secondary antibodies (goat anti-mouse or anti-rabbit IgG[f]~~; Vector Laboratories Inc.~~). Slides were counterstained with haematoxylin, dehydrated through graded ethanols and xylene and mounted in a xylene-based medium[g] ~~(DePex; Gurr BDH Chemicals Ltd)~~. For each dog a minimum of four sections were examined for each antibody.

For immunofluorescence, the basic protocol was the same for the peroxidase technique, without addition of H_2O_2, and the secondary antibody was applied for 60 min at room temperature in a dark humid chamber. Slides were washed in PBS (3 times for 5min), mounted and nuclear counterstained with DAPI mount (Vectashield). Positive controls included canine spleen (CD11c and CD45), lymph node (CD11c and CD45) and duodenum (Ki67, CD31, vWF, vimentin α-SMA and Smemb), and for negative controls the primary antibody was omitted. Images were taken using a light microscope with fluorescent capability[e] ~~(Leica DMRB)~~.

Image capture and analysis

For quantitative assessment (ImageJ cell counter plug-in[h]~~; National Institutes of Health~~) nine randomly selected (x400 magnification) non-overlapping images were digitally captured, beginning close to the valve edge (tip of leaflet) and moving back to the junction with the atrial myocardium ~~where the valve base (zone adjacent to the~~

annulus) covering the same region of interest for each valve, and the cells were then counted manually. Qualitative descriptive assessment only was carried out on the NovaRed stained sections (longitudinal and horizontal) and qualitative and quantitative assessment on the fluorescent labelled sections (longitudinal only).

Statistical analysis

Data were expressed as mean ± standard deviation of the mean. Since the sample size was small log transformation was undertaken to achieve normality, followed by the D'Agostino-Pearson normality test, and inferential statistical analysis applied using one-way analysis of variance (ANOVA) testing with a p value of <0.05. Where one-way analysis of variance (ANOVA) detected significant difference, inter-group differences were compared using the post-hoc Tukey Simultaneous test.

Results:

Gross and histological changes in myxomatous mitral valves from CKCS and non-CKCS were not appreciably different, and not dissimilar to previous reports [21,27].

Cellular changes in myxomatous mitral valve disease

Similar changes in the distribution of immunoreactive cells were noted for longitudinal and horizontal sections. In the normal mitral valves, most cells were vimentin positive and evenly distributed, and presumed to be quiescent VICs. In the diseased valves, vimentin positive cells were also evenly distributed, but the highest density was adjacent to the endothelial layer (Fig. 1). No cell staining was observed in any valve for the inflammatory cell markers CD11c or CD45, but positive staining was found in control lymph node. In normal mitral valves very few α-SMA or

SMemb+ cells were seen and these were typically located adjacent to the endothelium. In diseased valves α-SMA+ cells were generally found lying beneath the endothelium, clustering mostly at the distal free-edge with a few cells present in the valve stroma. SMemb positive cells were also found clustering surrounding the myxomatous areas and close to the distal free-edge, but there was positive staining throughout the leaflet depth. There were no clear differences comparing CKCS and the mixed breed dogs (Fig. 1). vWF+ endothelial cells were found along the whole leaflet length, but with areas of discontinuity in the diseased dogs. A consistent finding in both diseased groups (5/6 CKCS; 6/6 mixed breed) was clusters of vWF+ cells in the myxomatous sites away from the valve edge (Fig 2). No CD31+ cells were seen in any test or control sample. We have been unsuccessful in identifying CD31 positive cells in any canine paraformaldehyde fixed tissues, but have found this antibody to be effective in canine valve endothelial cell cultures.

Ki-67+ cells formed linear clusters typically at the leaflet tip, but also were distributed sparsely throughout the myxomatous valves of both groups (Fig 2). Staining appeared to be a combination of cytoplasmic and nuclear. This sparse distribution was somewhat similar to that seen for α-SMA and SMemb+ cells, but cell counting was not feasible. In affected valves, flattened elongated cells at the valve surface ~~(presumed to be VECs)~~ also showed positive staining for Ki-67.

Immunofluorescence; Qualitative and Quantitative Analysis

The total numbers of cells positive for α-SMA was significantly increased in the CKCS group compared to normal (Table 2) ($p<0.05$). SMemb+ cells were significantly increased in the two diseased groups compared to normal ($p<0.05$).

Vimentin+ cells made up the largest number in all valves, and cell numbers in both diseased valves approached twice that seen in normal valves (Table 2; Fig. 3). While the pattern of staining for α-SMA and SMemb at the valve edge was similar in both affected groups, only a few of those cells co-expressed both antigens (Fig. 3 & Fig. 4). In overtly myxomatous areas, the overall pattern of cellular staining was similar in the CKCS and mixed breed dogs.

Discussion:

The cavalier King Charles spaniel ~~(CKCS)~~ breed predisposition to MMVD is well recognised and heritability has a role in disease appearance and progression[4,5]. There are some CKCS-specific traits identified and while their association with MMVD can be unclear, it is reasonable to suggest that disease phenotype and pathology might be different to that seen in other dogs[7-11]. By assessing for a range of markers for inflammation, proliferation and mesenchymal cell phenotypic differentiation evidence was found that cell changes in the CKCS valve ~~are fundamentally the same~~ appear to be similar to that seen in mixed breed dogs.

There was no evidence of inflammatory cells in any of the samples examined and this is in agreement with the only other report [16]. Small numbers of macrophages and mast cells have been previously found in MMVD valves and there is an increased expression of some inflammatory cytokine transcripts in affected valves, but there still is no clear evidence that inflammation has an important role in this disease [17, 28,29].

Appearance of activated of α-SMA+ valve interstitial cells in canine MMVD is well recognised, particularly in the distal portion of the valve and close to the valve edge,

239 and this was again noted in the present study in all affected dogs [16, 17]. Increased α-
240 SMA+ cells numbers were seen in the two affected groups and were moderately
241 higher in the CKCS valves~~, but this could be a chance finding~~. Increased numbers of
242 α-SMA+ cells is dependent on disease severity and the dogs in the current study were
243 aged and had the most severe form of the disease [19]. Increased SMemb+ cell numbers
244 have also been previously reported and were found again to be increased in this study,
245 with a marginally higher number in the non-CKCS dogs [16]. The distribution of
246 Smemb+ cells in the valve stroma possibly identifies a cell population with
247 differentiation potential, but the presence of Ki-67 expression would suggest
248 proliferation is on-going as well. Lastly, using vimentin as a general mesenchymal
249 cell maker, total cell numbers in the two affected groups were similar and were
250 approximately twice that of the normal valves. Reports to date on changes in cells
251 numbers are either equivocal or conflicting, but this is likely to be based on the
252 counting techniques used. In myxoid stroma cell numbers decline, but overall cell
253 numbers increase and this is dominated by increased cell numbers in the atrialis layer
254 [15,21]. The current study furthermore confirms there is an overall increase in interstitial
255 cell numbers when the entire valve length is examined. However, it should be noted
256 the normal valves were not age-matched and increased cell numbers associated with
257 aging cannot be discounted. The lack of age-matched normal controls is a study
258 limitation, but it is understood that finding normal mitral valves in aged dogs is not
259 readily achievable.
260
261 While vimentin expression is widespread in many cell types, interstitial cells
262 expressing vimentin are generally considered to be a quiescent phenotype form of
263 VIC in the normal mitral valve [16, 17, 21]. In the diseased valve cells retaining vimentin

expression alone, or expressing one or both of the two activation/differentiation markers (α-SMA and SMemb), may represent an expanded population available for phenotypic alteration in response to appropriate triggers. There was an increased expression of the cell proliferation marker Ki-67 in the MMVD valves and this was most noticeable where there was the largest number of α-SMA positive cells close to the distal free-edge. This finding contrasts with the only other study where Ki-67 showed minimal expression in diseased valves [16]. Additionally the similar regional expression of Ki-67 with α-SMA+ cells ~~would~~ might suggest proliferation of activated myofibroblasts close to the valve edge is more likely than migration of these cells from deep in the valve stroma, and it would be reasonable to suggest this proliferation is in response to the endothelial changes and damage noted with MMVD [26]. Co-localisation staining would confirm if this was the case. Under normal circumstances VECs and VICs interact to prevent VIC activation and ~~VEC~~ endothelial-to-mesenchymal transition (EndoMT) (the process by which endothelial cells invade tissue and differentiate into a mesenchymal phenotype) thereby maintaining a quiescent state [30]. However, up-regulation of genes associated EndoMT is found in affected canine valves, suggesting changes in cellular homeostasis occurs with disease progression [30,31]. EndoMT is likely to be one mechanism that contributes to accumulation of α-SMA positive cells close to the endothelium.

Identification of cells positive for ~~a~~α-SMA and Smemb and the distribution of these cells has been previously reported, but the identification of co-localisation is a novel finding[16,17,21]. This co-localisation of α-SMA and SMemb in a small number of cells close to the valve edge identifies a population that have greater differentiation potential than those expressing α-SMA or SMemb alone, with Smemb having

289 important functions in cell adhesion and cell migration.~~.~~ Such cells are believed to
290 have greater phenotypic differentiation capability in response to injury[32]. In the case
291 of MMVD, a similar capacity for phenotypic versatility might exist where endothelial
292 damage has occurred.
293
294 VonWillebrand factor expression demonstrated the presence of the endothelium in all
295 valves and confirmed the loss of endothelial cells along some sections of affected
296 valve edges. Endothelial damage and denuding is now recognised to be a cardinal
297 feature of MMVD, and might be a major triggering event driving the phenotypic
298 changes seen with VICs and proliferation of aVICs close to the valve edge [2, 23, 24]. The
299 localised expression of vWF in cells within the stroma of the diseased valves was an
300 un-expected finding, suggesting either migration of endothelial cells or mesenchymal
301 transition of stromal VICs (mesenchymal to endothelial transition). The localisation of
302 Smemb+, vWF+ and Ki-67+ cells in the stroma might support the latter conclusion.
303 This finding might be due to extravasation during sample collection, but the number
304 of cells and consistency of the finding make this less likely. Successful staining for
305 CD31 would have been useful to clarify the endothelial identity or not of these cells,
306 as would double staining to identify co-localisation. Lastly, while there appears to be
307 a common pathological end-point when comparing MMVD in CKCSs and mixed
308 breed dogs this does not presume a shared pathogenesis, although that would not be
309 an unreasonable ~~to presume so~~ conclusion.
310
311 The main limitations of this study is the sample size (a recognized problem with
312 studies of this nature) and the technical problem of comparative sampling from
313 normal and diseased valves that have markedly different geometry. The laminated

structure of the normal valve compared to the loss of lamination in the disease valves is also a confounding factor. ~~Lastly, while there appears to be a common pathological end-point when comparing MMVD in CKCSs and mixed breed dogs this does not presume a shared pathogenesis, although it would not be unreasonable to presume so.~~

In conclusion, this study confirms that there is no evidence for inflammatory cell involvement in canine MMVD, that the cell changes ~~are similar~~ appear similar for CKCS as for other dogs, and that the changes in cell numbers in MMVD are possibly due to cell proliferation. This study suggests MMVD is not a heterogeneous disease, at least in terms of cellular changes and that the CKCS form of the disease differs only in its time of onset and speed of progression. However, the pathogenesis of MMVD is unknown and it is possible different mechanisms could result in the same end-stage findings. ~~However, for now it seems it is the temporal presentation and not the end-stage pathology that is likely to be the heritable feature of MMVD in the cavalier King Charles spaniel. Furthermore, it~~ From these studies it would be reasonable to presume that studies of any dog with MMVD are applicable to all dogs and breeds.

Acknowledgements:

The authors are indebted to the owners who have donated valve tissue from their pets to this study. Without their support this work would not have been possible. We are particularly indebted to the Cavalier King Charles Club of England for assistance in sourcing the CKCS material and their financial support of C-C Lu.

Conflict of Interest:

None of the authors of this paper has a financial or personal relationship with other people or organisations that could inappropriately influence or bias the content of the paper.

References:

1. Beardow AW, Buchanan JW. Chronic mitral valve disease in cavalier King Charles spaniels. 95 cases (1987-1991), J Am Vet Med Assoc 1993; 203:1023-1029.

2. Olsen LH, Mortensen K, Martinussen T, Larsson LI, Baandrup U, Pedersen HD. Increased NADPH-diaphorase activity in canine myxomatous mitral valve leaflets, J Comp Pathol 2003; 129:120-130.

3. Haggstrom J, Kvart C, Hansson K. Heart sounds and murmurs: changes related to severity of chronic valvular disease in the Cavalier King Charles spaniel, J Vet Intern Med 1995; 9:75-85.

4. French AT, Ogden R, Eland C, Hemani G, Pong-Wong R, Corcoran B, Summers KM.Genome-wide analysis of mitral valve disease in Cavalier King Charles Spaniels, Vet J 2012; 193:283-286.

5. Lewis T, Swift S, Woolliams JA, Blott S. Heritability of premature mitral valve disease in Cavalier King Charles spaniels, Vet J 2011; 188:73-76.

6. Davis B, Toivio-Kinnucan M, Schuller S, Boudreaux MK. Mutation in beta1-tubulin correlates with macrothrombocytopenia in Cavalier King Charles Spaniels, J Vet Intern Med 2008; 22:540-545.

7. Singh MK, Lamb WA. Idiopathic thrombocytopenia in Cavalier King Charles Spaniels, Australian veterinary journal 2005; 83:700-703.

8. Cowan SM, Bartges JW, Gompf RE, Hayes JR, Moyers TD, Snider CC, Gerard DA, Craft RM, Muenchen RA, Carroll RC. Giant platelet disorder in the Cavalier King Charles Spaniel, Exp Hematol 2004; 32:344-350.

9. Tarnow I, Kristensen AT, Texel H, Olsen LH, Pedersen HD. Decreased platelet function in Cavalier King Charles Spaniels with mitral valve regurgitation, J Vet Intern Med 2003; 17:680-686.

10. Pedersen HD, Mow T. Hypomagnesemia and mitral valve prolapse in Cavalier King Charles spaniels, Zentralbl Veterinarmed A 1998; 45:607-614.

11. Arndt JW, Reynolds CA, Singletary GE, Connolly JM, Levy RJ, Oyama MA.Serum serotonin concentrations in dogs with degenerative mitral valve disease, J Vet Intern Med 2009; 23:1208-1213.

12. Ljungvall I, Höglund K, Lilliehöök I, Oyama MA, Tidholm A, Tvedten H, Häggström J. Serum serotonin concentration is associated with severity of myxomatous mitral valve disease in dogs. J Vet Int Med 2013; 27: 1105–1112,

13. Hadian M, Corcoran BM, Bradshaw JP: Molecular changes in fibrillar collagen in myxomatous mitral valve disease, Cardiovasc Pathol 2010;19: 141-148.

14. Lewis T, Rusbridge C, Knowler P, Blott S, Woolliams JA. Heritability of syringomyelia in Cavalier King Charles spaniels, Vet J 2010; 183:345-347.

15. Watson PJ, Roulois AJ, Scase T, Johnston PE, Thompson H, Herrtage ME. Prevalence and breed distribution of chronic pancreatitis at post-mortem examination in first-opinion dogs, J Small Anim Pract 2007; 48:609-618.

16. Disatian S, Ehrhart EJ, 3rd, Zimmerman S, Orton EC. Interstitial cells from dogs with naturally occurring myxomatous mitral valve disease undergo phenotype transformation, J Heart Valve Dis 2008; 17:402-411.

17. Han RI, Black A, Culshaw GJ, French AT, Else RW, Corcoran BM. Distribution of myofibroblasts, smooth muscle-like cells, macrophages, and mast cells in mitral valve leaflets of dogs with myxomatous mitral valve disease, Am J Vet Res 2008; 69:763-769.

18. Rabkin E, Aikawa M, Stone JR, Fukumoto Y, Libby P, Schoen FJ. Activated interstitial myofibroblasts express catabolic enzymes and mediate matrix remodeling in myxomatous heart valves, Circulation 2001; 104:2525-2532.

19. Aupperle H, Marz I, Thielebein J, Schoon HA. Expression of transforming growth factor-beta1, -beta2 and -beta3 in normal and diseased canine mitral valves, J Comp Pathol 2008; 139:97-107.

20. Disatian S, Lacerda C, Orton EC. Tryptophan hydroxylase 1 expression is increased in phenotype-altered canine and human degenerative myxomatous mitral valves, J Heart Valve Dis 2010; 19:71-78.

21. Han RI, Black A, Culshaw G, French AT, Corcoran BM. Structural and cellular changes in canine myxomatous mitral valve disease: an image analysis study, J Heart Valve Dis 2009; 19:60-70.

22. SurachetpongS, JiranantasakT, Rungsipipat A, Orton EC. Apoptosis and abundance of Bcl-2 family and transforming growth factor b1 signaling proteins in canine myxomatous mitral valves. J Vet Cardiol 2013; 15: 171-180

23. Corcoran BM, Black A, Anderson H, McEwan JD, French A, Smith P, Devine C. Identification of surface morphologic changes in the mitral valve leaflets and chordae tendineae of dogs with myxomatous degeneration, Am J Vet Res 2004; 65:198-206.

24. Black A, French AT, Dukes-McEwan J, Corcoran BM. Ultrastructural morphologic evaluation of the phenotype of valvular interstitial cells in dogs with myxomatous degeneration of the mitral valve, Am J Vet Res 2005; 66:1408-1414

25. Mow T, Pedersen HD. Increased endothelin-receptor density in myxomatous canine mitral valve leaflets. J Cardiovasc Pharmacol. 1999; 34:254-60.

26. Han RI, Clark CH, Black A, French A, Culshaw GJ, Kempson SA, Corcoran BM. Morphological changes to endothelial and interstitial cells and to the extra-cellular

matrix in canine myxomatous mitral valve disease (endocardiosis). Vet J 2013; 197; 388–394.

27. Whitney JC. Observations on the effect of age on the severity of heart valve lesions in the dog, J Small Anim Pract 1974; 15:511-522.

28 Oyama MA, Chittur SV. Genomic expression patterns of mitral valve tissues from dogs with degenerative mitral valve disease, Am J Vet Res 2006, 67:1307-1318.

29. Zois~~a~~ NE, Moesgaard SG, Kjelgaard-Hansen M, Rasmussen CE, Falk T, Fossing C, Häggström J, Pedersen HD, Olsen LH. Circulating cytokine concentrations in dogs with different degrees of myxomatous mitral valve disease. Vet J 2012;192:106–111

30. Shaperoa K, Wylie-Searsa J, Levined RA, Mayer Jr. JE, Bischoff, J Reciprocal interactions between mitral valve endothelial and interstitial cells reduce endothelial-to-mesenchymal transition and myofibroblastic activation J Mol Cell Cardiol 2015; 80; 175–185.

31. Lu C-C, Liu M-M, Culshaw G, Clinton M, Argyle DJ, Corcoran, BM Gene network and canonical pathway analysis in canine myxomatous mitral valve disease: a microarray study. Vet J 2015; doi:10.1016/j.tvjl.2015.02.021 (in press)

32. Frangogiannis NG, Michael LH, Entman ML.Myofibroblasts in reperfused myocardial infarcts express the embryonic form of smooth muscle myosin heavy chain (SMemb), Cardiovasc Res 2000; 48:89-100.

470 Table 1. Antibody source and concentration used for IHC in canine mitral valves.
471

Primary and Secondary Antibodies	Origin	Dilution	Manufacturer	Catalogue No.
α-SMA	Mouse monoclonal	1:400	Sigma	A2547
SMemb	Rabbit polyclonal	1:1000	Abcam	Ab24761
Vimentin	Mouse monoclonal	1:1600	Sigma	V6389
vWF	Rabbit polyclonal	1:1000	Abcam	Ab6994
Ki-67	Rabbit polyclonal	1:200	Abcam	Ab15580
CD11c	Mouse monoclonal	1:100	Abcam	Ab76911
CD45	Mouse monoclonal	1:100	AbD Serotec	MCA2035S
CD31	Rabbit polyclonal	1:100	Abcam	Ab28364
Alexafluor 488	Goat anti-Mouse IgG (H+L)	1:100	Invitrogen	A10667
Alexafluor 568	Goat anti-Rabbt IgG (H+L)	1:100	Invitrogen	A11011
Biotinylated Antibody	Goat anti-Mouse IgG (H+L)	1:1000	Vector	BA-9200
Biotinylated Antibody	Goat anti-Rabbit IgG (H+L)	1:1000	Vector	BA-1000

472
473

474

475 Table 2. Comparison of cell numbers (mean +/-SD) positive for α-smooth muscle
476 actin (α-SMA), embryonic smooth muscle myosin (Smemb) and vimentin in mitral
477 valves of cavalier King Charles spaniels (CKCS n=6), mixed breed dogs (n=6) with
478 myxomatous mitral valve disease (MMVD) and normal mixed breed dogs (n=4). Data
479 log transformed. * Significantly different from control group $P<0.05$.
480

	α-SMA (Mean±SD)	Smemb (Mean±SD)	Vimentin (Mean±SD)
CKCS n=6	33.95±12.13*	23.13±5.72*	40.52±18.41
non-CKCS n=6	25.7±2.67	29.55±3.06*	46.95±17.65
Control n=4	10.75±2.95	14.53±3.96	26.75±7.24

481

482

Figure 1. Immunohistochemistry of myxomatous mitral valves from cavalier King Charles spaniels (CKCS; Left Panel A, B & C) and non-CKCS (Right Panel D, E & F). Photomicrographs for immunostaining of vimentin (A&B) alpha-smooth muscle actin (α-SMA; C&D) and myosin heavy chain-10 (Smemb; E&F) in the distal zone. There is a similar aggregation pattern of α-SMA, SMemb, and vimentin in CKCS and non-CKCS with positive cells forming linear clusters along the valve edge most noticeable with α-SMA . Magnification α-SMA, SMemb, Vimentin 20x, bar = 50μm.

Figure 2. Photomicrographs of Von Willebrand Factor (vWF) immunostained myxomatous mitral valves (vWF; right panel A-C) and Ki-67 (left panel D-F). (A) Continuous layer of endothelium showing expression of vWF, compared with (B) interrupted endothelium. (C) Spindle-shaped vWF positive cells clustering in the spongiosa. (D) Multi-layered Ki-67 positive cells aggregating in the myxomatous region at the distal end of mitral valve leaflets. (E) Clusters of Ki-67 positive cells in the spongiosa. (F) Single layer of endothelial cells showing positive staining for the proliferation marker Ki-67. Magnification (A-D) 20x, Bar = 50μm, (E) (F) 40x, Bar = 25 μm.

Figure 3. Fluorescence photomicrograph of cavalier King Charles spaniel myxomatous mitral valve, taken at the level of the valve edge. Immunofluorescence staining for alpha-smooth muscle actin (α-SMA), myosin heavy chain-10 (Smemb), Vimentin, and 4-6-diamidino-2- phenylindole (DAPI, blue) nuclear counterstaining. Magnification 40x, scale = 25 μm.

Figure 4. Double fluorescence photomicrographs of cavalier King Charles spaniel myxomatous mitral valve, taken at the level of the valve edge. Alpha-smooth muscle actin (α-SMA; green) and myosin heavy chain-10 (Smemb; red). There is a different staining pattern of α-SMA and SMemb positive cells. The merged photomicrographs show occasional cells co-expressing α-SMA and SMemb (arrows). Magnification 40x, scale = 25 μm.

Footnotes:

c. ABC Elite Kit, Vector Laboratories Inc.

d. AlexaFluor488 and 568, Invitrogen

e. Leica-DMRB

f. Vector Laboratories Inc.

g. DePex; Gurr-BDH Chemicals Ltd

h. National Institutes of Health

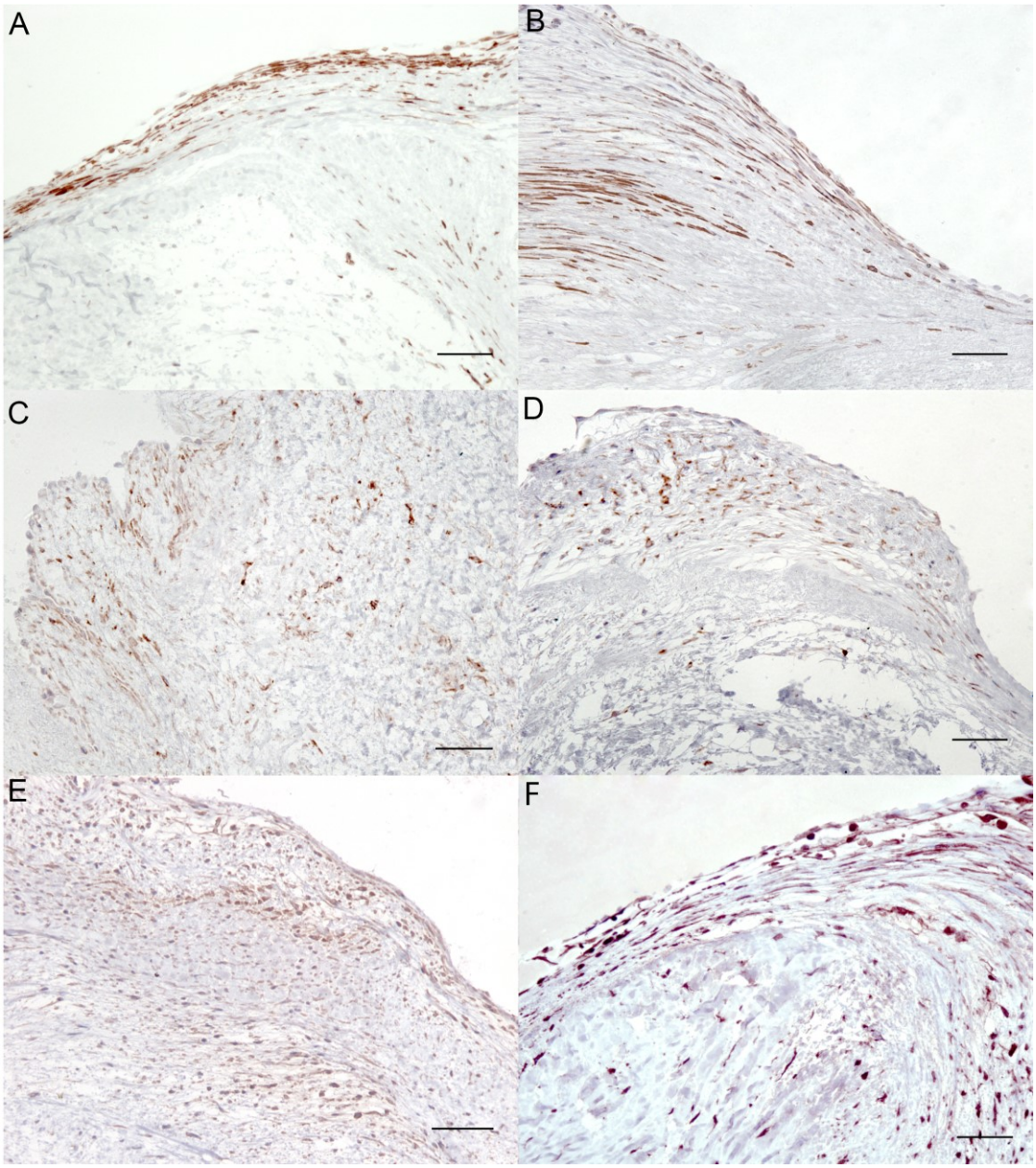

Figure1

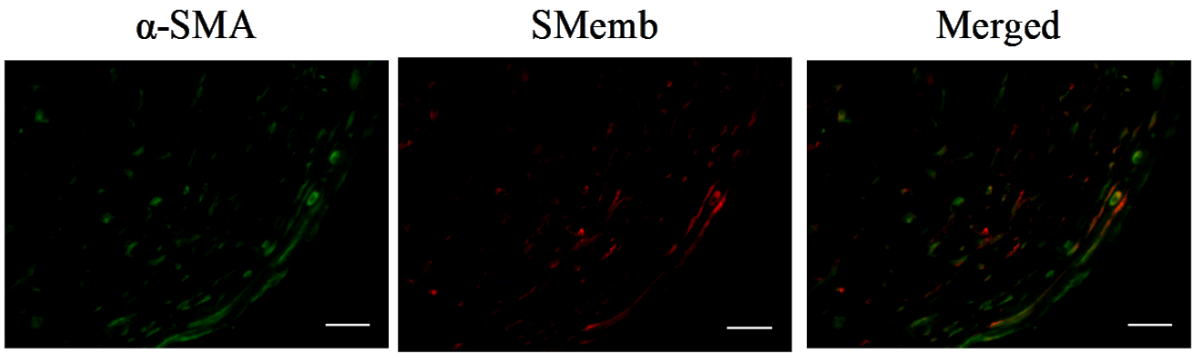

Figure 2

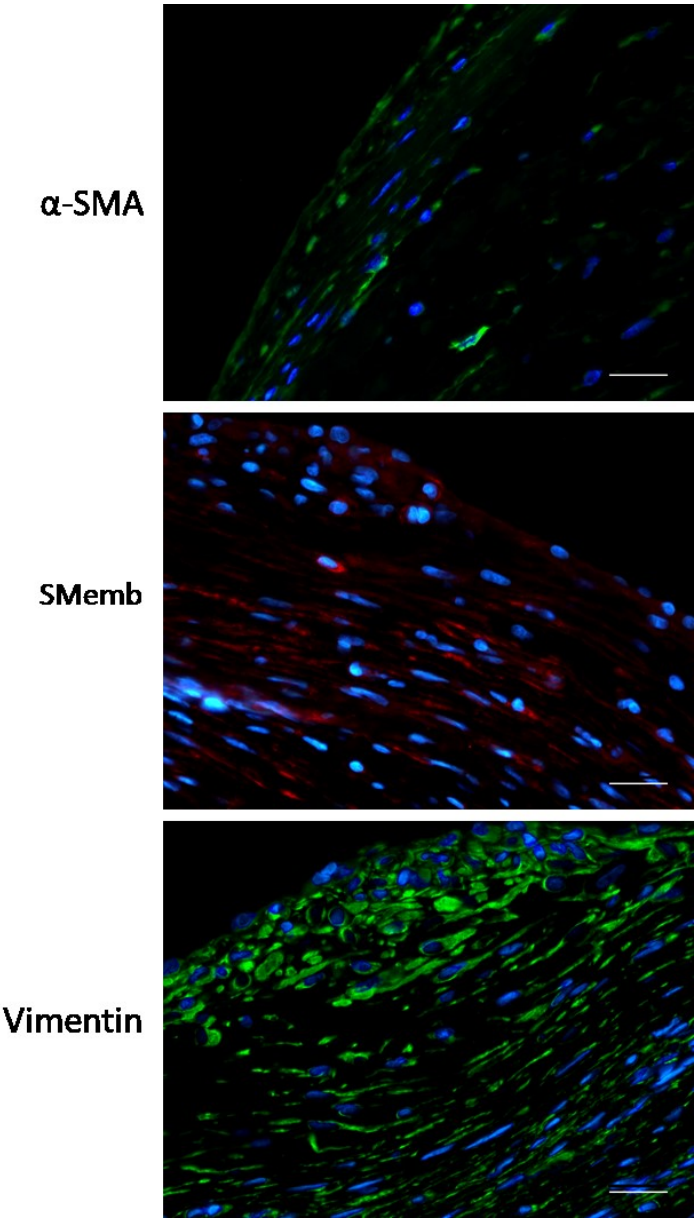

526

527 Figure 3

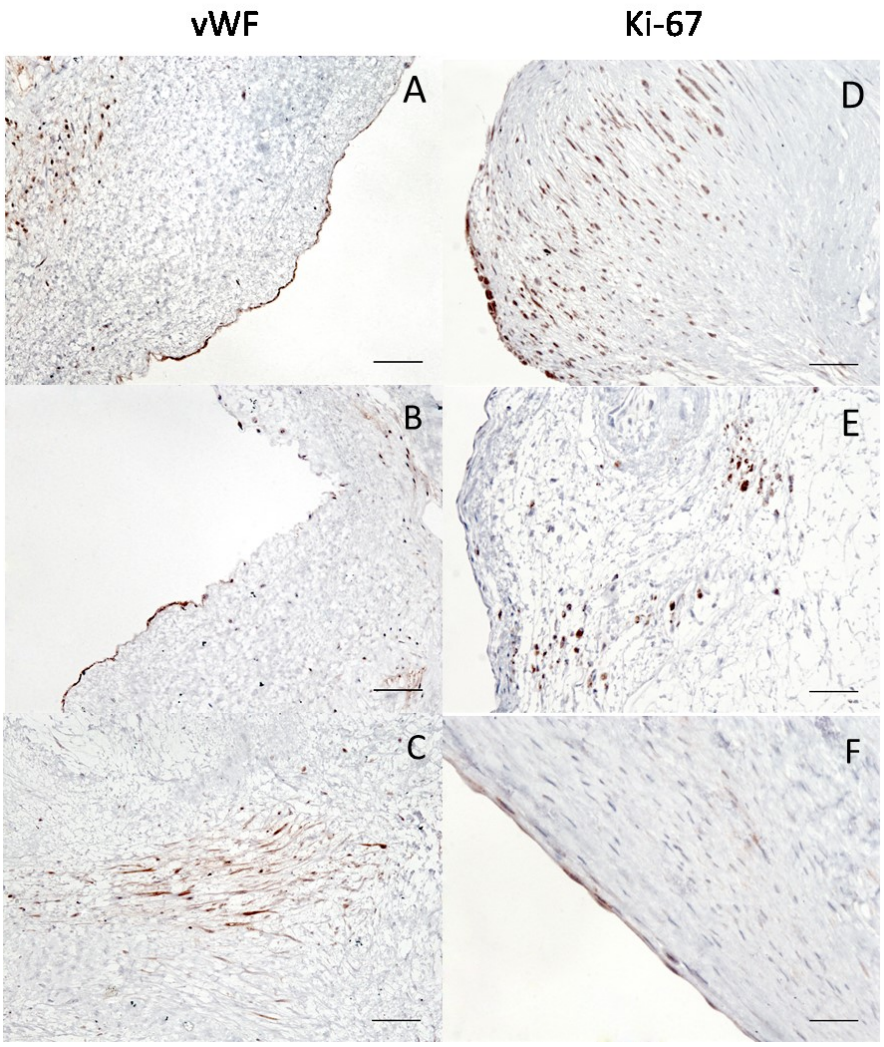

Figure 4